$3d$ x-ray-absorption lines and the $3d^9 4f^{n+1}$ multiplets of the lanthanides

B. T. Thole,* G. van der Laan,* and J. C. Fuggle
Laboratory for Physical Chemistry, University of Nijmegen, Toernooiveld, NL-6525 ED Nijmegen, The Netherlands

G. A. Sawatzky
Institute for Physical Chemistry, University of Groningen, Nijenborgh 16, NL-9747 AG Groningen, The Netherlands

R. C. Karnatak and J.-M. Esteva
Laboratoire pour l'Utilisation du Rayonnement Electromagnétique, F-91405 Orsay Cédex, France and Unité No. 040 775 associée au Centre National de la Recherche Scientifique, Université de Paris—Sud, F-91405 Orsay Cédex, France

(Received 1 April 1985)

We have measured and calculated the $3d$ ($M_{4,5}$) absorption spectra for all the rare-earth metals, as well as the full $3d^9 4f^{n+1}$ multiplets for the early and late rare earths. The quality of agreement between theory and experiment is excellent, except for Sm. In x-ray-absorption spectroscopy (XAS), only dipole selected lines are seen but all multiplet effects can be observed in x-ray photoemission spectroscopy. The line shapes and $3d$-$4f$ interactions are discussed. Our results provide an improved basis for use of the $3d$ XAS spectra for studies of "mixed-valence" systems.

I. INTRODUCTION

There is a long history of studies of the $3d$ ($M_{4,5}$) x-ray-absorption spectra (XAS) of rare earths dating back at least to Lindberg's study in 1931.[1] However, many factors combine to make a new and systematic study of these spectra by both experimental and theoretical methods desirable. These include advances in experimental technique and the use of synchrotron radiation, advances in the uses of computers,[2] and new recognition of the role that XAS has to play in studies of solid-state and mixed-valence properties of rare earths.[3] Further motivation comes from the recognition of interesting relaxation of dipole selection rules in electron energy-loss spectra near the core-hole threshold[4] in certain x-ray photoemission spectroscopy (XPS) peaks,[5] and the interest in observation of strong variation of photodesorption cross sections for photon energies near x-ray-absorption edges in rare earths.[6]

The x-ray-absorption spectra of the rare earths in the region of the $3d$ levels have strong sharp peaks near the edges due to $3d^{10}4f^n \rightarrow 3d^9 4f^{n+1}$ transitions. These absorption lines dwarf the true $3d \rightarrow 6p$ edges and the absorption cross sections are $\sim 10^{-16}$ cm^2, which is too high to permit absorption studies by conventional thin film or powder techniques, such as used for the $L_{2,3}$ edges of the rare earths[7] (RE). Thus until quite recently the best XAS studies of the rare earths were made by measurements on evaporated rare-earth films sandwiched between two carbon films[1,8–11] with all the dangers of reactions with the films, although self-absorption methods have also been used. These methods are tedious and cannot compete with the use of synchrotron radiation and photoyield methods, which gives good quality spectra in a matter of minutes.

Line saturation effects are expected to be present in the yield spectra when the photon penetration depth becomes comparable to the electron escape depth. In such situations, as in the case of $M_{4,5}$ spectra of RE, the analysis of experimental line shapes and widths needs a careful data treatment for an estimation of true line shapes and widths and their comparison with theoretical predictions.

A second major advance has been in the use of computers to calculate the shape of the $3d^9 4f^{n+1}$ multiplet effects. These are strong because of the strong $4f$ localization. There have been several calculations of the multiplet structure in individual elements[11–15] and Demekhin[12] calculated spectra of Eu^{2+}, Gd^{3+}, Tb^{3+}, Dy^{3+}, and Ho^{3+} using only the states of highest multiplicity. However, there are now computers available capable of dealing with even the most complex $d^9 f^{n+1}$ multiplet structure in intermediate coupling. We felt that calculations were desirable for the XAS multiplet structure for each of the possible ground-state configurations for each of the rare earths because some rare earths form compounds with more than one valence, or even with configurational fluctuations. This has been done. Finally we have, where practical, calculated the full $d^9 4f^{n+1}$ multiplet structure which is important for understanding the origin of some satellite structure in electron-initiated spectroscopic methods like x-ray emission, energy-loss spectroscopy, appearance potential spectroscopies, etc.

The organization of this paper is as follows. In Sec. II we describe briefly the computational method and in Sec. III we give experimental details. In Sec. IV we give the experimental and computational results and discuss their general significance and their relation to other measurements.

II. CALCULATIONS

The complete atomic multiplet calculations in intermediate coupling, including all the states of the configura-

TABLE I. Electrostatic and exchange parameters used in the calculation. (a) F and G integrals used (reduced to 80% of HF values, all values in eV). (b) Parameters related to the spectral simulation.

(a)

		$3d^{10}4f^n$				$3d^9 4f^{n+1}$								
n		$F^2_{(f)}$	$F^4_{(f)}$	$F^6_{(f)}$	ζ_f	$F^2_{(f)}$	$F^4_{(f)}$	$F^6_{(f)}$	$F^2_{(fd)}$	$F^4_{(fd)}$	$G^1_{(fd)}$	$G^3_{(fd)}$	$G^5_{(fd)}$	ζ_d	ζ_f
La^{3+}	0								5.65	2.53	3.78	2.21	1.52	6.80	0.092
Ce^{4+}	0								6.56	3.00	4.53	2.65	1.83	7.44	0.119
Ce^{3+}	1				0.087	10.10	6.35	4.57	5.99	2.71	4.06	2.37	1.64	7.45	0.107
Pr^{4+}	1				0.115	10.28	7.13	5.15	6.85	3.16	4.78	2.80	1.93	8.14	0.136
Pr^{3+}	2	9.78	6.14	4.41	0.103	10.48	6.59	4.74	6.31	2.87	4.33	2.53	1.75	8.14	0.124
Nd^{3+}	3	10.18	6.39	4.60	0.114	10.84	6.81	4.91	6.62	3.03	4.59	2.69	1.85	8.88	0.135
Pm^{3+}	4	10.56	6.63	4.77	0.136	11.18	7.03	5.07	6.92	3.19	4.84	2.83	1.96	9.67	0.160
Sm^{3+}	5	10.92	6.85	4.93	0.155	11.51	7.24	5.21	7.21	3.34	5.09	2.98	2.06	10.51	0.180
Sm^{2+}	6	10.02	6.25	4.48	0.141	10.68	6.68	4.80	6.70	3.08	4.67	2.73	1.89	10.51	0.165
Eu^{3+}	6	11.27	7.07	5.09	0.175	11.84	7.44	5.36	7.50	3.48	5.33	3.12	2.16	11.41	0.202
Eu^{2+}	7	10.40	6.49	4.66	0.161	11.03	6.90	4.95	7.00	3.23	4.92	2.88	1.99	11.41	0.187
Gd^{3+}	7	11.60	7.28	5.24	0.197	12.16	7.64	5.50	7.77	3.63	5.56	3.26	2.25	12.36	0.226
Tb^{4+}	7	12.66	7.99	5.76	0.237	13.17	8.31	5.99	8.51	4.01	6.18	3.63	2.51	13.36	0.268
Tb^{3+}	8	11.93	7.49	5.39	0.221	12.47	7.84	5.64	8.04	3.77	5.79	3.40	3.35	13.37	0.251
Dy^{3+}	9	12.25	7.69	5.53	0.246	12.77	8.03	5.78	8.31	3.91	6.02	3.53	2.44	14.44	0.278
Ho^{3+}	10	12.57	7.88	5.67	0.273	13.07	8.21	5.91	8.57	4.04	6.24	3.66	2.53	15.57	0.307
Er^{3+}	11	12.87	8.08	5.81	0.302	13.37	8.40	6.04	8.83	4.18	6.46	3.79	2.62	16.78	0.338
Tm^{3+}	12	13.18	8.26	5.94	0.333				9.09	4.31	6.68	3.92	2.71	18.05	0.371
Tm^{2+}	13				0.314									18.05	
Yb^{3+}	13				0.366									19.39	

(b)

	ΔE_{AV} (eV)	σ_{Gauss} (eV)	$q_{3/2}$	Shift Δ (eV)	α_{SO}[a]	$A_{5/2}$[b] (Å^{2}eV)	$A_{3/2}$[b] (Å^{2}eV)	λ (Å)
La^{3+}	841.5	0.25	8	−3.4	95.6	1.090	1.701	29
Ce^{4+}	892.7	0.25	8	−2.9	99.0	1.231	1.991	
Ce^{3+}	889.3	0.25	8	−2.9	99.0	1.242	1.461	51
Pr^{4+}	941.2	0.30	6	−3.9	95.3	1.360	1.701	
Pr^{3+}	938.1	0.30	6	−3.9	95.3	1.328	1.237	53
Nd^{3+}	987.8	0.30	7	−3.9	96.3	1.395	1.034	57
Pm^{3+}	1038.6	0.30	7	−4.0	100	1.437	0.825	
Sm^{3+}	1090.4	0.35	7	−4.4	100	1.437	0.642	92
Sm^{2+}	1088.3	0.35	7	−4.4	100	1.224	0.480	
Eu^{3+}	1143.2	0.35	7	−4.7	98.8	1.370	0.514	
Eu^{2+}	1141.2	0.35	7	−4.7	98.8	0.991	0.542	86
Gd^{3+}	1197.1	0.35	6	−4.2	98.3	1.094	0.586	62
Tb^{4+}	1254.4	0.40	9	−4.2	99.1	1.190	0.622	

TABLE I. (*Continued*).

	ΔE_{AV} (eV)	σ_{Gauss} (eV)	$q_{3/2}$	(b) Shift Δ (eV)	α_{SO}[a]	$A_{5/2}$[b] (Å^2 eV)	$A_{3/2}$[b] (Å^2 eV)	λ (Å)
Tb^{3+}	1252.0	0.40	9	−4.2	99.1	1.075	0.384	119
Dy^{3+}	1308.1	0.40	8	−5.0	99.6	1.010	0.221	121
Ho^{3+}	1365.2	0.40	8	−5.5	99.3	0.888	0.108	107
Er^{3+}	1423.4	0.40		−5.0	99.4	0.699	0.056	114
Tm^{3+}	1482.7	0.40		−3.8	99.2	0.488	0.019	126
Tm^{2+}	1481.2	0.40		−3.8	99.2	0.241	0	
Yb^{3+}	1543.1	0.40		−4.8	100	0.256	0	258

[a]Percent reduction of the Hartree-Fock value spin-orbit required to fit to the experiment.
[b]Cross section integrated over the peak group.

tion $4f^n$ for the ground state and $3d^9 4f^{n+1}$ for the excited state, have been performed for all the rare-earth ions for all ionization states known in the solid state. These calculations could be made using Cowan's program[2] on a Digital Equipment Corporation VAX 11/750 computer using about 1 Mbyte ($10^6 \times 8$ binary digits) of central memory. The values of the parameters were obtained by Cowan's atomic Hartree-Fock (HF) program with relativistic corrections.[2] This calculation was done for the average of the $4f^n$ ground-state configuration and the average of the $3d^9 4f^{n+1}$ excited-state configuration with all lower shells filled. The electrostatic and exchange parameters were all scaled down to 80% of their HF value. These scaled values are given in Table I. The scaling accurately described the total spread of the lines in the $3d_{3/2}$ and $3d_{5/2}$ peaks in La^{3+}, Ce^{3+}, and Tm^{3+}. The same scaling was satisfactory for the other rare earths. More detailed optimization was considered unnecessary because the uncertainty of the measurement and the neglect of configuration interaction make fully optimized values artificial and unphysical. The spin-orbit parameter for the $3d$ orbital was adjusted by the factor α_{SO} [Table I(b)] to give the correct distance between the $3d_{5/2}$ and $3d_{3/2}$ peaks. The HF values for the spin-orbit parameters are given in Table I as well as the HF values for the difference in the average energy of the two configurations. This value had to be shifted by Δ, also given in Table I. The absolute intensities of the possible dipole transitions were convoluted by a Lorentz line shape of width $2\Gamma_{5/2}$ full width at half maximum (FWHM) for the $3d_{5/2}$ peaks and by a Fano line shape of $2\Gamma_{3/2}$ and asymmetry parameters $q_{3/2}$ for the $3d_{3/2}$ peaks. The resulting spectrum was finally convoluted by a Gaussian line shape with standard deviation σ_{Gauss}. The values used for the linewidth are discussed in Sec. IV C. The total integrated intensities of the $3d_{3/2}$ and $3d_{5/2}$ peaks ($A_{3/2}$ and $A_{5/2}$) in Table I have been calculated from the theoretical spectrum. These values may be used to obtain concentration ratios of a mixture of, e.g., two valence states of a rare-earth ion.

To obtain the absorption length, at the maximum of the spectrum, it is necessary to broaden the line spectra with the physical (noninstrumental) contributions to the line

TABLE II. Major absorption peak energies in eV, experimental error ±0.3 eV unless otherwise stated.

Element	$3d_{5/2}$	$3d_{3/2}$	Difference
La	834.2	850.5	16.3
Ce	882.3	889.6	17.3
Pr	929.6	949.3	19.7
Nd	978.4	1000.2	21.8
Sm	1079.0	1103.9	24.9
Eu	1128.1	1155.0	26.9
Gd	1148.1	1213.2	29.1
Tb	1238.4	1270.1	31.7
Dy	1292.9	1326.9	34.0
Ho	1348.1	1385.1	37.0
Er	1404.9	1446.3	41.4
Tm	1463.0±1	1508.1±1	45.1
Yb	1519.6±1		

shapes (e.g., lifetime broadening 2Γ and Fano effects) to obtain σ, the maximum absorption cross section. λ is then $1/(\sigma\rho)$ where ρ is the density of atoms. As described later, there are uncertainties in the 2Γ values and other physical effects on the line shapes. Nevertheless we think it useful to list the λ values obtained from our theoretical simulations in Table I, although these may be up to $\sim 50\%$ too high, because our simulations include instrumental broadening. It is not generally realized just how low the values of λ are.

III. EXPERIMENTAL

Pure rare-earth metals supplied by Johnson and Matthey were used for most of these investigations. For Tb, of which we had none, $TbAl_2$ was substituted and Yb_2O_3 was substituted for Yb as the latter has 14 $4f$ electrons atom^{-1} and yields no $3d \rightarrow 4f$ adsorption signal. For other elements oxides were not used because the surfaces of oxide powders may be contaminated with hydroxides, higher or lower valence oxides and carbonates, and because XAS in the photoyield mode is surface sensitive. The samples were scraped clean and measured in ultrahigh vacuum (typically 3×10^{-10} Torr).

For the experiment, radiation from the ACO [Anneau de Collision, LURE (Laboratoire pour l'Utilisation du Rayonnement Electromagnétique)] synchrotron ring was filtered using a Be window to remove low-energy radiation, and to reduce background, and then monochromatized using a double crystal beryl monochromator.[16] The resolution of the monochromator varies between ~ 380 meV at 830 eV and ~ 700 meV at 1500 eV.[16] The flux from the monochromator was checked using the photoyield from elements which have no structure in the spectral region of interest (e.g., $_{13}$Al). The only sharp structure is a "glitch" at ~ 896 eV, for which we have corrected in the Ce spectra, and an absorption at ~ 1079 eV due to Na impurities in the Beryl crystals. There are changes in transmitted flux from ~ 800 to ~ 1600 eV, due to the properties of the synchrotron and the dispersion of the monochromator which are not serious for our purposes. We also found the flux to vary slowly with energy on a scale of ~ 100 eV in the low-energy region (800—900 eV) in a way that was dependent on the precise crystal adjustment. We could not correct for this and hence one should not attribute significance to the M_4:M_5 peak ratios in La and (to a lesser extent in Ce).

The spectral reported here were recorded with an x-ray incidence angle of 50°—70° to the surface normal and recording the yield of electrons with a single Channeltron in the pulse-counting mode.

IV. RESULTS

A. Comparison with earlier experimental spectra

The observed and calculated spectra are given in Fig. 1. The observed spectra show significant differences with respect to those measured by Fischer and Baun.[9] Thus, apart from improved resolution in our experiments we find that many extra, satellite lines present in earlier data for Ce, Pr, Nd, Sm, Eu, Gd, Tb, Dy, and Tm are not found in ours. These extra lines are a characteristic of the self-absorption method in which one is dependent on the identity of the emission spectra at two different energies of the exciting electron beam. However, the emission spectra are not necessarily the same because in near-threshold excitation dipole selection rules do not apply and with high-energy beams double-ionization satellites become important. The agreement between our data and those for RE oxides reported by Kaindl *et al.*[17] is better and the resolution is comparable. There are, of course, major differences for Ce and Eu where the oxides used by Kaindl *et al.* (CeO_2 and Eu_2O_3) have valences and initial-state configurations differing from those of the pure metals. We also find sharper peaks for Ho and Tm than these authors report. As our monochromator should have similar performance we attribute the differences to differences in experimental geometry (see Sec. IV C) or to contamination of their oxide surfaces.

B. General features

The spectral shapes in Fig. 1 are unlike normal "edge" structures in that they have sharp peaks attributable to the $3d \rightarrow 4f$ transitions which led early workers to suggest that they were better described as "line" absorptions. The spectra features are in two groups whose separation corresponds roughly to the $3d_{3/2}$-$3d_{5/2}$ spin-orbit splitting (see Table II). Note, however, that the individual groups show considerable structure which is due to coupling of the spin and orbit moments of the $3d$ and $4f$ electrons. The spectra must be described in intermediate coupling and hence the designations $3d_{3/2}$ (M_4) and $3d_{5/2}$ (M_5), while convenient, are only approximate. It is interesting to note that the $3d_{3/2}$ and $3d_{5/2}$ line shapes in the full multiplet are rather similar, especially for Nd and Pr, but the observed XAS line shapes are quite different. This is because the dipole matrix elements give appreciable intensity to quite different parts of the total multiplet.

The integrated intensity of the M_4 absorption lines is comparable to that of the M_5 lines in the early rare earths, but its relative intensity rapidly decreases in the heavier rare earths (see Table I). The origin of the effect is certainly in the selection rules because the ratio of numbers of levels in the $d_{5/2}$ and $d_{3/2}$ states is always 3:2. However, the basic physics is not easy to visualize in intermediate coupling. For La and Yb an explanation where spin-orbit coupling is the dominant interaction and $\Delta j = +1$ is the dominant channel is not completely unphysical. For La the "weight" of the $3d_{3/2} \rightarrow 4f_{5/2}$ excitation is $4\times6=24$ and that of the $3d_{5/2} \rightarrow 4f_{7/2}$ is $6\times8=48$. Other possibilities are forbidden so that the ratio of the $3d_{3/2}$:$3d_{5/2}$ peaks is 1:2. Our full calculation in intermediate coupling yields 1.09:1.70. For Yb the only $4f$ hole has $4f_{7/2}$ character so that only the $3d_{5/2} \rightarrow 4f_{7/2}$ excitation is possible and only the $3d_{5/2}$ line should be observed. If spin-orbit coupling were the dominant interaction the $4f_{5/2}$ states would be filled first and only the $3d_{5/2}$ lines would be observed for all the late rare earths. This is not in agreement with experiment but the general trend that the $3d_{3/2}$:$3d_{5/2}$ ratio decreases across the rare-

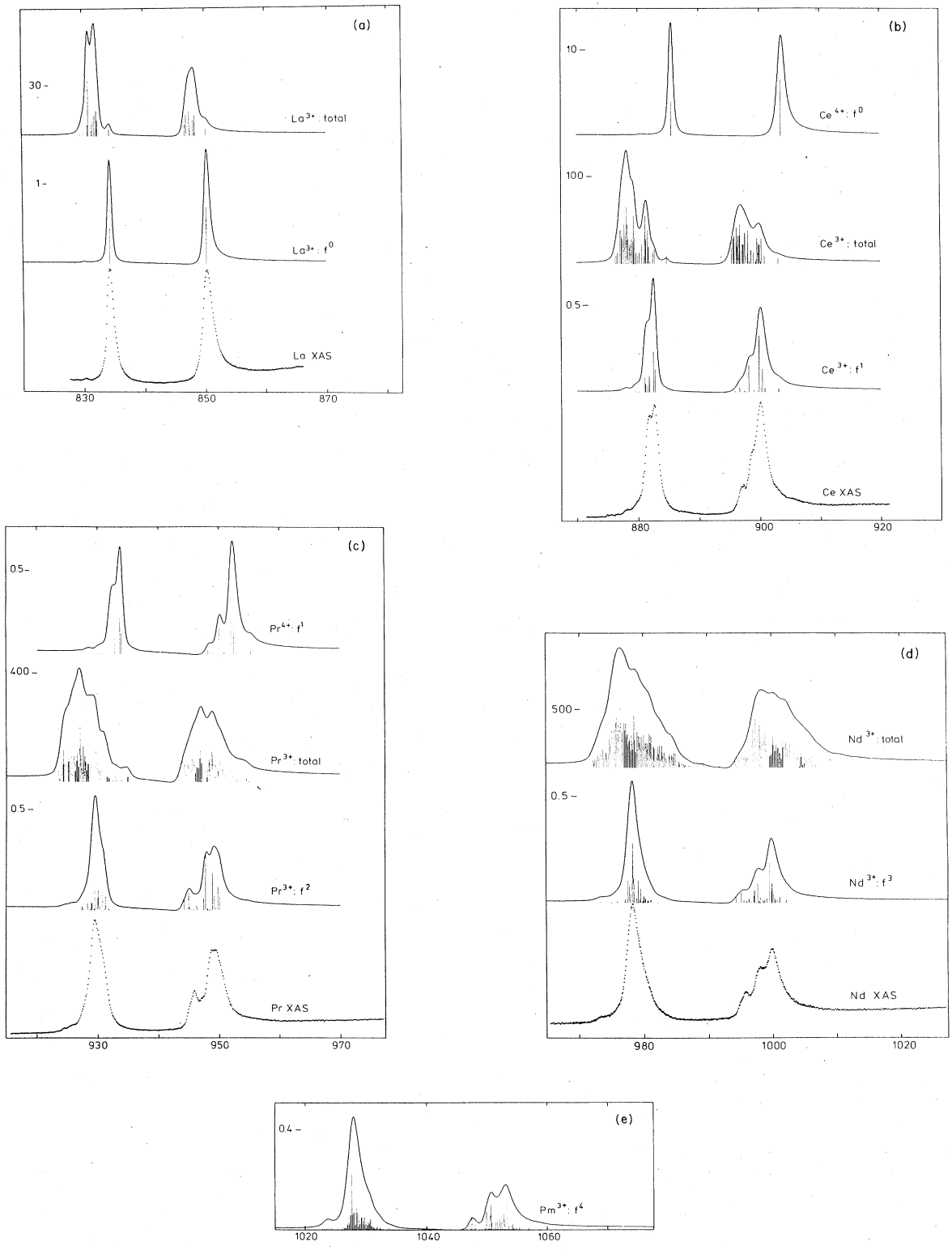

FIG. 1. Spectra of the rare-earth metals. The spectra labeled XAS are the experimental curves. The label f^n denotes the theoretical dipole excitation spectrum from the Hund's rule ground level of the configuration f^n to the levels of d^9f^{n+1}. The spectrum labeled "total" gives each level of d^9f^{n+1} with weight $2J+1$. The horizontal axes gives the excitation energy in eV. The experimental spectra have an unknown vertical scale. The scale of the theoretical spectra is indicated at the left. The dipole spectra give the absorption cross section σ in Å^2, the "total" spectra give the density of states in numbers of atomic levels per eV for the curves. The vertical lines have been normalized; close lying lines have been added.

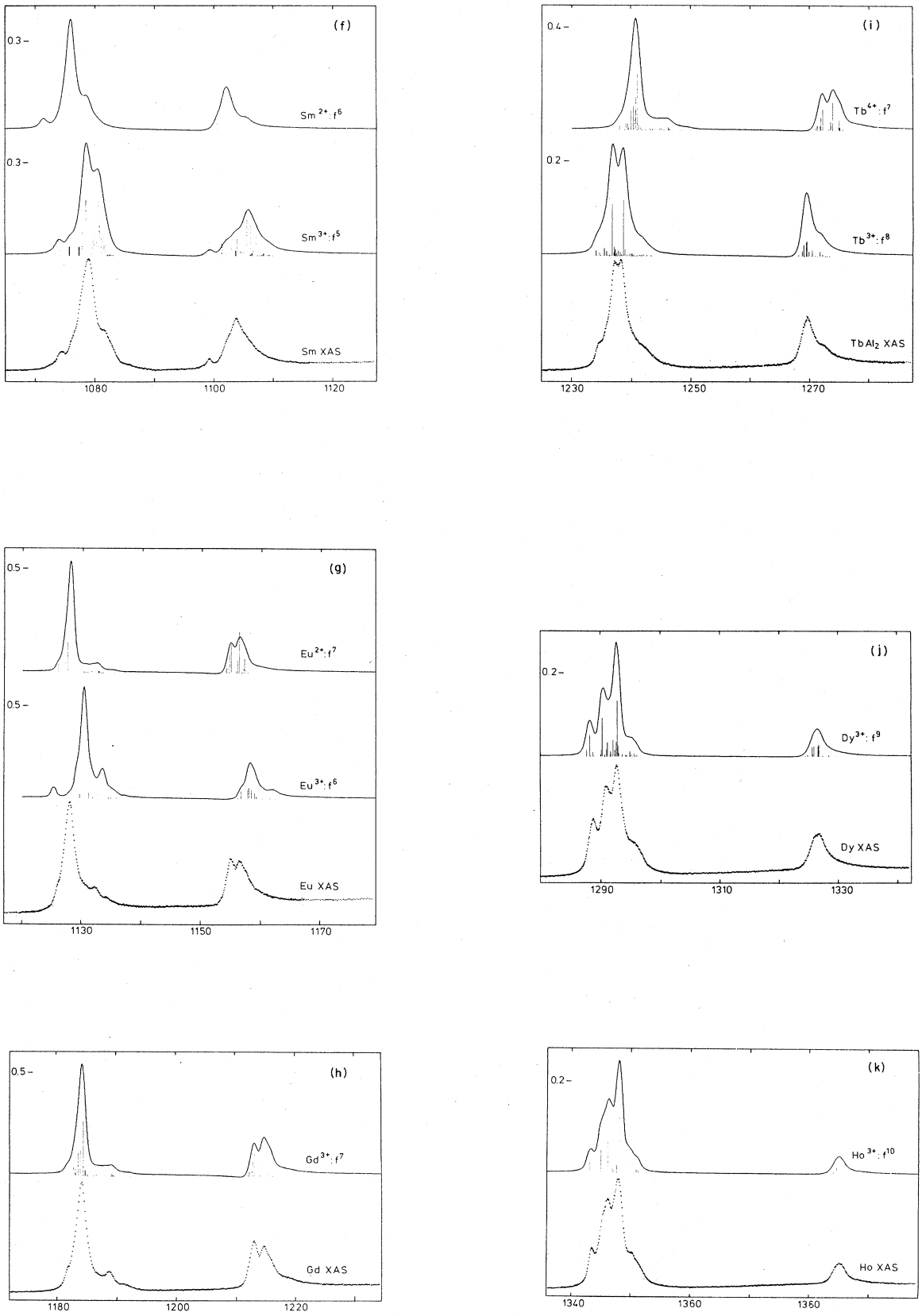

FIG. 1. (*Continued*).

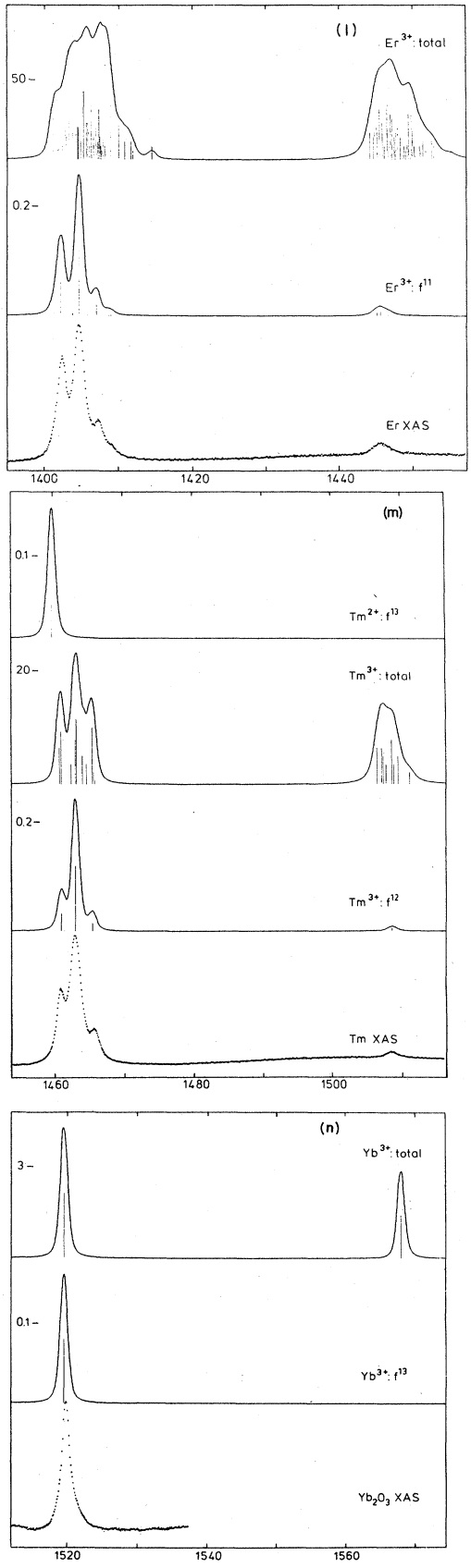

FIG. 1. (*Continued*).

earth series is probably related to a tendency for the occupied $4f$ levels in the ground state to have more $4f_{5/2}$ character than the empty states.

The $3d$ lifetime broadening of the $3d$ levels derived from our measurements ranges from $2\Gamma \approx 0.4$ eV for $La3d_{5/2}$ to $2\Gamma \approx 1.2$ eV for $Tm3d_{3/2}$. This is not large. However, although the radiative transition rates we calculate are large, they can still only account for a few percent of the lifetime broadening so that even here Auger processes are the predominant $3d$ hole decay channel.

C. Saturation effects

Two experimental effects immediately suggest some saturation effects in some of our data: (1) in many spectra the main peaks are experimentally weaker with respect to the small multiplet lines than calculated, (2) in elements like La, with a very simple XAS spectrum, we observe that a curve fitted to the wings of the peaks overestimates the observed peak intensity (this effect is not illustrated in detail here).

In the photoyield method one usually collects all photoelectrons, including secondaries. In a simple model for x-ray absorption in the photoyield mode we would have

$$Y = A\int_0^\infty e^{-x/(\lambda\cos\theta)}dx/(\lambda\cos\theta)e^{-x/d}$$
$$= Ad/(d+\lambda\cos\theta)\ ,$$

where A is the number of electrons produced per photon, which run in the direction of the surface, θ is the angle of incidence of the x-rays, λ is the absorption length, and d is the escape depth of the electrons (suitably averaged). When λ is large, this is approximately equal to $Ad/(\lambda\cos\theta)$. When λ is of the order of d, there is saturation. The maximum possible yield is A. The Tm^{3+} spectrum can approximately be obtained from the theoretical spectrum if we assume that the highest peak is reduced about 40% by saturation effects and thus here $d/(\lambda\cos\theta) \approx 1.5$. Assuming that $\cos\theta \approx 0.5$ and using $\lambda_{Tm} = 126$ Å [Table I(b)], we estimate d to be 65–115 Å for our experiments. From clear shoulders in the spectra of other rare earths we obtained values ranging from 15 to 115 Å with a distribution strongly peaked around 60 Å. Such values are not unreasonable in view of experimental data on thin layers.[18] Assuming that d does not vary much over the rare earths, we estimate that d is probably between 50 and 75 Å. Thus, for example, the equal intensities of the two strong La peaks could be due to saturation effects. Because of this assumed saturation, the experimental FWHM is larger than the true 2Γ value. Therefore we decided to choose σ and Γ for the experimental and lifetime broadening not by optimizing the fit, but to choose them such that the amount of structure was reproduced. We believe that values for the total lifetime broadening (2Γ) increase across the lanthanide series. Values of $\Gamma_{5/2}$ as low as 0.2 eV for La, 0.3 eV for Yb and $\Gamma_{3/2} = 0.4$ eV for La, 0.6 eV for Tm, seem most realistic (We did actually use slightly different values to simulate the experiments in order to show the multiplet structure well.) The values of Γ we find most realistic are lower than those in the literature, where saturation effects have

not been treated.[19–23]. The Fano parameter q for La and Ce may also not be accurate because of the saturation. In other elements the error is probably within 10%.

The saturation effects here are significant, although they do not negate the whole experiments. A fuller study of these effects, using various angles of incidence is desirable. For the future it would also be desirable to use some simple energy selection of the photoelectrons, for their average escape depth λ is dependent on their kinetic energy.

D. Multiplet effects

The total $3d^9 4f^{n+1}$ multiplet structure is very complex, and the total numbers of levels runs into thousands for many elements in the middle of the rare-earth series. Dipole selection rules greatly reduce the number of states which can be reached from the ground-state $3d^{10}4f^n$ configuration term, but even this does not produce simple spectra. Thus using $\Delta j = 0, \pm 1$ selection rules we find that the number of final-state levels that can be reached increases from 3 in La to 53 in Ce, to 200 in Pr and to 1077 in Gd. In the later rare earths, where the number of f holes is reduced, it falls again to 4 in Tm and 1 for Yb^{3+}. Natural linewidths (2Γ) due to lifetime broadening of the $3d_{5/2}$ level are ~ 0.4 eV for La and 0.6 eV for Yb while the $M_{3/2}$ linewidths are ~ -0.8 eV in La and ~ 1.2 eV for Tm. Thus it is not possible to resolve all the multiplet lines in the $3d$ XAS spectra except for La, Tm, and Yb. Nevertheless the multiplet effects do lead to significant structure in the XAS curves and this is clearly observed in the spectra and the calculated curves.

In general, most multiplet calculations published to date have relied upon bar diagrams to represent the calculated spectra. We have preferred to broaden and add the individual contributions as it gives a clearer picture of the degree of agreement. The agreement between theory and experiment is excellent except for a few minor features. The first notable disagreement does not always show up well in the global pictures we present, but we do find that the small shoulders in the wings of the main peaks are generally higher than calculated. As discussed in Sec. IV C, this is typical for saturation effects and may be explained by the exceptionally high absorption cross section in the rare earths. The second notable problem is the disagreement between calculated and observed spectra for Sm. The discrepancy in the Sm M_5 ($3d_{5/2}$) line shape is much larger than for the other elements. We will consider this point separately in Sec. IV K.

To compare our calculated spectra with those in the literature we must return to the line diagrams. We find diagrams very similar to those found for XAS of La, Ce, Er, and Tm by Sugar *et al.*[11,13,14] and by Bonnelle *et al.* for Eu and Gd.[15] When comparing our results with Demekhin's work[12] we find reasonable correspondence between the line diagrams for La, but not for Gd, Tb, Dy, Ho, Er, and Tm. For instance, in Gd^{3+} our calculation indicates a small weight in a very large number of lines on the high-energy side of the main $3d_{5/2}$ and $3d_{3/2}$ lines. This weight adds up to recognizable shoulders in the calculated spectra. Here this may be because Demekhin neglects all but the terms of highest multiplicity. In other cases, such as Er or Tb there are differences in the number of major lines he calculates but his paper does not give enough details for us to determine the reason for the discrepancy.

E. Comparison with energy-loss spectra

Netzer *et al.*[4] have found that at ~ 1000 eV above threshold a reflection electron energy-loss spectrum is equivalent to an XAS spectrum, but that near threshold the dipole selection rules break down and the peaks of the full multiplet are observed. For the early rare earths this extra structure comes on the low-energy side of the dipole-allowed peaks, as our calculations indicate. For the heavy rare earths we predict that extra intensity should be observed on the high-energy side, as shown in Fig. 1 for Er and Tm, and in Yb the $3d_{3/2}$ line should become visible.

F. The position of the $3d \rightarrow 4f$ lines with respect to the $3d \rightarrow$ VB edges

A $3d$ electron can be excited to the $4f$ or the valence-band (VB) levels,[24] i.e.,

$$3d^{10}4f^n(\mathrm{VB})^x \rightarrow 3d^9 4f^{n+1}(\mathrm{VB})^x \quad (1)$$

or

$$3d^{10}4f^n(\mathrm{VB})^x \rightarrow 3d^9 4f^n(\mathrm{VB})^{x+1}\,, \quad (2)$$

whereby the transition (2) of lowest energy corresponds to the edge for direct excitation of an electron into valence states as conceived in early work,[25,26] where screening due to an f electron was not considered. The relative energy of processes (1) and (2) are important for interpretation of the $3d_{3/2}$ line shapes[23] and for interpretation of XPS spectra.[5,27,28] However, it is not trivial to observe this energy difference directly in XAS spectra because process (2) is very weak. Further, as described below, the relative energies of processes (1) and (2) depends on the effective Coulomb interaction between the $3d$ hole and the $4f$ electron, U_{ac}. To determine U_{ac} we must utilize data from XPS and bremsstrahlung isochromat spectroscopy (BIS).

Let the ground state of the rare-earth ion in the metal have a configuration $3d^{10}4f^n(\mathrm{VB})^x$.[24] Then the $4f^{n+1}$ configuration has an energy Δ^+ which can be measured by bremsstrahlung isochromat spectroscopy.[29] Usually several peaks are observed in BIS of the lanthanides corresponding to the various $4f^{n+1}$ states which may be observed by addition of an electron to the $4f^n$ ground state. It is convenient to define an average value of the BIS peak positions Δ^+ as shown in Fig. 2 for Ce where Δ^+ is approximately 5 eV.[29,30]

Now consider the XPS spectrum shown in the lower part of Fig. 2. The lowest energy $3d_{5/2}$ hole state is actually one corresponding to a $3d^9 4f^2(\mathrm{VB})^x$ state at ~ 877 eV in the spectrum.[5,27,28] At higher energies the XPS spectrum shows first more intensity due to excitation to the higher energy $3d^9 4f^2$ states and then the major peak due to the $3d^9 4f^1(\mathrm{VB})^{x+1}$ states centered at ~ 883.7 eV.[31] Thus from XPS we can derive that the $4f^{n+1}$ states

are actually an energy $\Delta^- \sim 5$ eV lower than the $4f^n$ states which correspond to the true edges in XAS. Transposing this information on to the XAS spectrum of Ce we note that the $3d^{10}4f^n(\mathrm{VB})^x \rightarrow 3d^9 4f^1(\mathrm{VB})^{x+1}$ edge energy is slightly to the high BE side of the $4f^2$ multiplet line structure observed experimentally for both the $3d_{5/2}$ and $3d_{3/2}$ regions. A similar result has been recorded for La.[5]

Note now that the bulk of the $3d^9 4f^2$ multiplet states is not observed in XAS and that there are many Δ^- and Δ^+ values. The energy by which the $4f^{n+1}$ level is lowered with respect to a valence level at E_F may be defined as $U_{ac} = \Delta^- + \Delta^+$ but, as shown in Fig. 2, one could actually choose many values of both Δ^+ and Δ^-. The particular value chosen must, in fact, depend on the use to which it is put. The average value of Δ^- from $3d$ XAS of Ce is ~ 2 eV so that for Ce the value of U_{ac} appropriate to a BIS-XAS combination is ~ 7 eV. Using BIS, XPS, and XAS data we arrive at $U_{ac} \sim 6$ eV for La, ~ 6 eV for Pr, and ~ 6 eV for Nd. Larger values of U_{ac} are appropriate to an XPS-BIS combination because XPS selection rules allow a different distribution of weight in the $3d^9 4f^{n+1}$ final states.[3]

G. Line shapes and the $3d \rightarrow 6p$ edges

The M_4 $(3d_{3/2})$ edge has an asymmetric appearance with an obvious tail to higher energy in most of the elements studied. In elements, from Nd to Ho this can be partially explained by the presence of many multiplet lines with low weight on the high-energy side of the lines [indeed the same phenomena is often found on the high-energy side of the M_5 $(3d_{5/2})$ lines]. However, there is an additional effect in the M_4 $(3d_{3/2})$ lines associated more or less directly with the $3d_{5/2} \rightarrow$VB (valence-band) excitations which overlap the $3d_{3/2} \rightarrow 4f$ excitations. Motais *et al.*[22] have suggested that the asymmetry in the $_{57}$La M_4 $(3d_{3/2})$ line is due to the onset of a steplike edge due to the excitation of a $^3D_1$ line and an ionization of $5p$ subshell electron. These authors argue that the energy coincidence of this double excitation-ionization transition and M_4 $(3d_{3/2})$ threshold is responsible for the enhancement of the transitions to continuum states beyond the M_4 $(3d_{3/2})$ threshold. It is rather difficult to extend this argument to other higher RE. For these cases such energy coincidence cannot be reconciled with the much slower variation of the $5p$ ionization energy compared to the M_4 $(3d_{3/2})$—M_5 $(3d_{5/2})$ separation along the RE series.

The $3d \rightarrow$VB excitations have weak strength and are identified with difficulty because dipole selection rules restrict this excitation to the $3d \rightarrow np$ channel where $n = 6$ dominates near the edge. This channel is weak, not only because of the low $3d \rightarrow np$ cross section per p hole, but also because near threshold the empty valence-band states have mostly $5d$ character with a little $6s$. The np character increases with energy above E_F. In the rare earths, the $3d$ spin-orbit splitting is larger and the $3d_{3/2}$ lines need not obscure the $3d_{5/2} \rightarrow$VB structure. In some elements, such as Tm, a broad, weak absorption is seen ~ 15 eV above the $3d_{5/2}$ line and this may be the $3d_{5/2}$ continuum with which the $3d_{3/2}$ lines interact to give a Fano line shape.

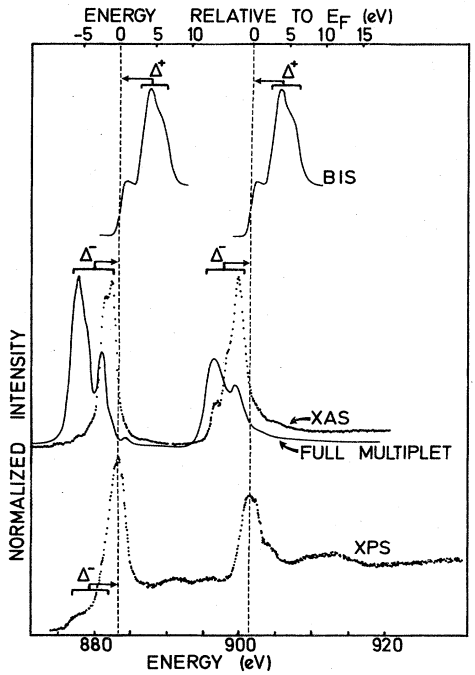

FIG. 2. Top, BIS spectra of Ce; middle, XAS and full $d^9 4f^2$ multiplet for Ce; lower section, XPS spectrum of Ce. This combination of data is used to determine the strength of interactions between a $3d$ hole and the $4f$ electrons.

H. La

The La $3d$ XAS spectrum exhibits just two lines in the $3d_{5/2}$ region ($^3P_1$ and $^3D_1$) and one in the $3d_{3/2}$ region ($^1P_1$). It provides a good case for analysis of the line profiles if saturation effects can be properly treated. We find a lifetime broadening of only ~ 0.4 eV most realistic. This is only approximate, but 2Γ is clearly lower than previously assumed: indeed it is probably the narrowest core-hole state known at such high energies[20] and as such it deserves more detailed study. Its width certainly seems to be as narrow as theoretical estimates would suggest.[19]

I. Ce

Ce is one of the most studied rare earths because of its interesting solid-state properties. There have also been many studies of the spectroscopic properties mostly seeking to clarify the role of the $4f^1(\mathrm{VB})^3$ and $4f^0(\mathrm{VB})^4$ configurations in the ground state. The general conclusion of all these studies is that the weight of the $4f^0(\mathrm{VB})^4$ configuration in the ground state is never larger than $\sim 30\%$ but that the hybridization between the $4f$ state and the valence levels is not negligible.

We find that for γ-Ce itself the observed XAS spectrum corresponds very closely to the multiplet structure calculated for the $3d^9 4f^2$ configuration when a $3d^{10}4f^1(^2F_{5/2})$ ground state is assumed. In a separate paper we consider the effect of mixing of $^2F_{7/2}$ character

into the ground state.[32] The lines due to the Ce $3d^9 4f^1$ configuration appear when the $4f^0$ configurations play a role in the ground state. No Ce compound gives an XAS spectrum corresponding to the pure $3d^9 4f^1$ multiplet which should resemble that of La. Not even the chemically 4-valent CeO_2,[17,33,34] whose ground-state configuration is nominally $4f^0$, gives the simple 3-line spectrum. This is presumably because very strong hybridization of the $4f$ level not only causes shift of spectral weight from the $4f^1$ to the $4f^2$ peaks, but also cause the $4f^1$ and $4f^2$ states to mix in the final state.[35]

The separation of the Ce $4f^1$ and Ce $4f^2$ multiplets has not been adjusted in the calculated spectra for Ce in Fig. 1 and is only ~ 3 eV, while in the experiments the separation was ~ 5 eV.[3] This is very respectable agreement for the energy difference in two total energy calculations but is an indication that the calculated multiplets must normally be shifted into alignment with experiment before they can be utilized to interpret spectra of mixed-valence lanthanide materials.

J. Pr, Nd, and Pm

For Pr and Nd the shape of the observed spectra agrees well with that calculated for Pr^{3+} and Nd^{3+}. As in Ce the full $3d^9 4f^{n+1}$ multiplet is shifted a little to lower energy with respect to the dipole-selected part of the multiplet. This is borne out by experiment, as for Ce: in XPS spectra the observed BE of the Pr $3d^9 4f^3$ feature is centered at 927.0 eV, and the Nd $3d^9 4f^4$ feature is at 975.3 eV (Ref. 27), and in both cases this is ~ 2 eV below the center of gravity of the absorption lines. Pr^{4+} ions are known to exist in oxides and oxide salts[34] but have not yet been investigated. Our calculations show that the XAS multiplet structure should be quite distinctive from that of Pr^{3+}. Pm, having an unstable nucleus, is not generally available for experimental studies.

K. Sm

Sm metal is considered to be trivalent although divalent and mixed-valent Sm compounds do exist with a contribution of the $4f^6$ configuration to the ground state. The spectrum of Sm metal is very similar to that published for Sm_2O_3 (Ref. 17) which is clearly trivalent with the $4f^5$ configuration. Nevertheless we find agreement between the observed Sm XAS spectrum and the calculated ($3d^{10}4f^5 \rightarrow 3d^9 4f^6$) transition spectrum poorer than for any other element studied: the M_5 peak has most intensity in a single (broad) peak, rather than the doublet calculated, and while the small M_4 peak at ~ 1099 eV is correctly placed, the major M_4 peak is at ~ 2 eV higher energy than the ~ 1004 found. There are anomalies in the crystal reflectivity in the Sm M_5 region due to Na impurities. Correction for these anomalies would decrease the intensity of the main M_5 line at 1079 eV by $\sim 40\%$ and improve agreement with experiment. However, this does not explain all the differences in the M_5 region and makes no correction to the M_4 discrepancies. The experimental Sm^{2+} $M_{4,5}$ spectrum published by Kaindl *et al.*[17] is very similar to our calculated Sm^{2+} spectrum, which suggests that our multiplet calculations are reasonable. Also those results confirm the ~ 2.5 eV shift between the major 2^+ and 3^+ peaks (although there is a difference in absolute energy scales between their measurements and ours) which again suggests that the discrepancies cannot be due to presence of Sm^{2+} material in our sample.

We are thus left with the conclusion that there is a discrepancy between the Sm^{3+} XAS spectra measured and calculated. We think that one possible explanation for the discrepancy lies in the small separation (~ 100 meV) between the ground-state Sm $4f^5\ {}^6H_{5/2}$ configuration and the first excited state Sm ${}^6H_{7/2}$.[36] In a spherical configuration these are not allowed to mix but this may no longer be true in the lower symmetry of the solid. This could be confirmed by studies of other Sm environments or studies of gaseous Sm. Certainly we caution against excessive emphasis on interpretation of the $M_{4,5}$ XAS line shapes of Sm compounds until the puzzle of the Sm^{3+} line shape is solved.

L. Eu and Gd

The XAS spectra of Eu and Gd are very similar to each other and to the calculated $3d^{10}4f^7 \rightarrow 3d^9 4f^8$ spectra. There is also good agreement with the spectra of Gd_2O_3 published by Bonnelle *et al.*[15] and by Kaindl *et al.*[17] The calculations of Bonnelle *et al.* failed to explain the intensity on the high-energy side of the M_5 lines. The shoulders we calculate at ~ 1132 eV for Eu and 1189 eV for Gd are actually not due to intensity in a few lines, but are due to very small weights in well over 100 multiplet lines. It is not surprising that these were missed in the earlier work. We still do not reproduce the shape of the shoulders and the weak peaks at ~ 1132 eV in Eu and ~ 1189 eV in Gd. The failure to reproduce this little peak is probably symptomatic of the accuracy of the approximations in our calculations. We reject any explanation on the basis of Eu^{3+} in the Eu spectrum because the peak position does not match Eu^{3+} and because the same feature is found in Gd and this would require the presence of Gd^{4+} (Gd $4f^6$) in the Gd and this species is not chemically stable.

The calculated XAS spectrum for Eu^{3+} is very similar to that of Eu_2O_3.[37,17] Further, we note that the calculated separation of the main features o the Eu^{2+} and Eu^{3+} spectrum is very similar to that found by Kaindl *et al.*,[17] although comparison of the figures shows a difference of ~ 1 eV between his experimental excitation energies and ours.

M. Tb

Tb is another of the rare earths which is known to exist in two valences. We lacked a sample of Tb metal and had to be satisfied with one of $TbAl_2$. This is very closely related to that calculated for Tb^{3+} ($4f^8$). The spectrum of Tb^{4+} ($4f^7$) is similar in shape to that of Eu^{2+} and Gd^{3+}. No experimental XAS spectra of a Tb^{4+} compound have been published but the broad structures found in $Tb_{11}O_{20}$ are compatible with a sum of our calculated 3^+ and 4^+ spectra with appropriate weightings.[17]

N. Dy, Ho, and Er

Besides giving examples of the good agreement between theory and experiment, these elements deserve little further specific comment. The experimental spectrum of Ho_2O_3 (Ref. 17) is much less sharp than that which we present for Ho which may be due to saturation effects or to degradation of the oxide surface.

O. Tm

We obtain good agreement between the calculated Tm^{3+} spectrum and that calculated by Sugar[14] as well as with the experimental result. Our experimental result is marginally sharper than that of Kaindl *et al.*[17] for Tm_2O_3 which may be due to degradation of the oxide. The Tm^{2+} ($4f^{13}\rightarrow 4f^{14}$) XAS spectrum is calculated to show a single M_5 line at lower energy than the Tm^{3+} M_5 line. This result is compatible with a study of mixed-valence Tm compounds.[3,38,39] Our own results certainly support the assertion that the Tm spectra can be used for studies of Tm mixed valence, although saturation effects and the apparent chemical sensitivity of the broadening of the Tm^{3+} ($f^{12}\rightarrow f^{13}$) line shapes, indicated by a comparison of our work with Ref. 38, suggest that some literature estimates of the error limits on valences determined by XAS are too optimistic.

P. Yb

Yb metal itself is divalent and has the f^{14} configuration. It should thus exhibit no $3d\rightarrow 4f$ absorption line and Combley *et al.*[40] attributed the very weak line they measured to divalent impurities. In Yb_2O_3 we find a single line at 1519.6 eV due to the $3d^{10}4f^{13}_{7/2}\rightarrow 3d^{9}_{5/2}4f^{14}$ transition. Transitions to the $3d^{9}_{3/2}4f^{10}$ state, shown in the full multiplet calculation, are forbidden. We did not try to check the $3d_{3/2}$ (M_4) line region carefully because Al in the beryl crystals of the monochromator absorbs in the Yb M_4 region.

V. CONCLUDING REMARKS

We have shown that the measured $3d$ absorption lines of the rare earths have complex structure due to the $d^9 4f^{n+1}$ multiplet. With the exception of Sm, these multiplet structures can be adequately explained by calculations based on Hartree-Fock calculations of the initial and final states and an atomic-state calculation in intermediate coupling to give the weights of the individual final-state multiplet lines. As in other systems the Slater F and G integrals must be reduced to $\sim 80\%$ of the Hartree-Fock values to obtain good agreement with experiment. We conclude from an analysis of the line shapes in those spectra with simple multiplet structure (La and Tm) that the intrinsic linewidths are smaller than assumed heretofore. The spectra show saturation effects near peak absorption, even in photoyield mode.

In XAS dipole selection rules hold and only a part of the full $d^9 4f^{n+1}$ multiplet is observed. This is not true for the $d^9 4f^{n+1}$ lines in XPS because the "screening" $4f$ electron is taken from the valence band of the solid in such a way as to allow higher Δj terms.[27–32] It is also not true in ELS with low primary beam energies[4] so that the "full multiplet" can be observed in those experiments. For the light rare earths the center of gravity of the full multiplet is calculated and observed to be at lower energy than the dipole-allowed terms.

In the rare earths the energy of the $4f^{n+1}$ level is lowered with respect to E_F by the core-hole potential U_{ac}. It is only an approximation to use a single U_{ac} value because of the complicated multiplet effects in both the $d^{10}4f^{n+1}$ and $d^9 4f^{n+1}$ configurations.

We calculate shifts in the $3d$ absorption energies as a function of f count due to the differences in final state f^n and f^{n-1} configuration energies. This can be used as a probe of mixed valence, as already pointed out in the literature.[3,17,38] However, because of the overlap in the contributions from different configurations, a knowledge of the multiplets of the individual configurations is desirable.

ACKNOWLEDGMENTS

We are grateful to the Laboratoire pour l'Utilisation du Rayonnement Electromagnétique (LURE) technical staff for their valuable aid and to the Group Anneau du Laboratoire de l'Accélérateur Linéaire, Orsay, for their help in operating the machine. We also thank R. Cowan for allowing us access to his computer codes. We also thank J. Keppels and the Kernforschungsanlage (KFA) Jülich for technical assistance. This work was supported in part by the Netherlands Foundation for Chemical Research (Stichting Scheikundig Onderzoek Nederland) with financial aid from the Netherlands Organization for the Advancement of Pure Research (Nederlandse Organisatie voor Zuiver-Wetenschappelijk Onderzoek), and by the Centre Nationale de la Recherche Scientifique (CNRS), France.

*Present address: Institute for Physical Chemistry, University of Groningen, Nijenborgh 16, NL-9747 AG Groningen, The Netherlands.

[1]E. Lindberg, Nova Acta Reg. Soc. Sci. Upsaliensis **7**, 7 (1931).

[2]R. Cowan, J. Opt. Soc. Am. **58**, 808 (1968); *The Theory of Atomic Structure and Spectra* (University of California Press, Berkeley, 1981).

[3]J. C. Fuggle, F. U. Hillebrecht, J.-M. Esteva, R. C. Karnatak, O. Gunnarsson, and K. Schönhammer, Phys. Rev. B **27**, 4637 (1983).

[4]J. A. D. Matthew, G. Strasser, and F. P. Netzer, Phys. Rev. B **27**, 5839 (1983); F. P. Netzer, G. Strasser, and J. A. D. Matthew, Phys. Rev. Lett. **51**, 211 (1983).

[5]J.-M. Esteva, R. C. Karnatak, J. C. Fuggle, and G. A. Sawatzky, Phys. Rev. Lett. **50**, 910 (1983).

[6]B. E. Koel, G. M. Loubriel, M. L. Knotek, R. H. Stulen, R. A. Rosenberg, and C. C. Parks, Phys. Rev. B **25**, 5551 (1982).

[7]L. Azaroff and D. M. Pease, in *X-Ray Spectroscopy,* edited by L. Azaroff (McGraw-Hill, New York, 1974), pp. 289ff.

[8]See, e.g., K. C. Rule, Phys. Rev. **68**, 246 (1945); H. F. Zandy,

Proc. R. Soc. London, Ser. A **65**, 1015 (1952); E. A. Stewardson and J. E. Wilson, Proc. Phys. Soc. London, Sect. A **69**, 93 (1956).
[9]D. W. Fischer and W. L. Baun, J. Appl. Phys. **38**, 4830 (1967).
[10]T. M. Zimkina, V. A. Fomichev, S. A. Gribovskii, and I. I. Zhukova, Fiz. Tverd. Tela (Leningrad) **9**, 1447 (1967) [Sov. Phys.—Solid State **9**, 1128 (1967); **9**, 1490 (1967) [**9**, 1163 (1967)].
[11]C. Bonnelle, R. C. Karnatak, and J. Sugar, Phys. Rev. A **9**, 1920 (1974).
[12]V. F. Demekhin, Fiz. Tverd. Tela (Leningrad) **16**, 1020 (1974) [Sov. Phys.—Solid State **16**, 659 (1974)].
[13]J. Sugar, Phys. Rev. A **6**, 1764 (1972).
[14]J. Sugar, Phys. Rev. B **5**, 1785 (1972).
[15]C. Bonnelle, R. C. Karnatak, and N. Spector, J. Phys. B **10**, 795 (1977).
[16]M. Lemonnier, O. Collet, C. Depautex, J.-M. Esteva, and D. Raoux, Nucl. Instrum. Methods **152**, 109 (1978).
[17]G. Kaindl, G. Kalkowski, W. D. Drewer, B. Perscheid, and F. Holtzberg, J. Appl. Phys. **55**, 1910 (1984).
[18]J.-M. Esteva, R. C. Karnatak, and J. P. Connerade, J. Electron Spectrosc. Relat. Phenom. **31**, 1 (1983).
[19]E. J. McGuire, Phys. Rev. A **5**, 1043 (1972).
[20]J. C. Fuggle and S. F. Alvarado, Phys. Rev. A **22**, 1615 (1980).
[21]J. P. Connerade and R. C. Karanatak, J. Phys. F **11**, 1539 (1981).
[22]P. Motais, E. Belin, and C. Bonnelle, J. Phys. F **11**, L169 (1981).
[23]R. C. Karnatak, J.-M. Esteva, and J. P. Connerade, J. Phys. B **14**, 4747 (1981).
[24]Note that by x we mean the average number of valence electrons per atom in the ground state.
[25]W. Kossel, Z. Phys. **1**, 119 (1920).
[26]F. K. Richtmyer, S. W. Barnes, and E. Ramberg, Phys. Rev. **46**, 843 (1934).
[27]G. Crecelius, G. K. Wertheim, and D. N. E. Buchanan, Phys. Rev. B **18**, 6519 (1978).
[28]J. C. Fuggle, M. Campagna, Z. Zolnierek, R. Lässer, and A. Platau, Phys. Rev. Lett. **45**, 1597 (1980).
[29]J. K. Lang, P. A. Cox, and Y. Baer, J. Phys. F **11**, 121 (1981).
[30]F. U. Hillebrecht, J. C. Fuggle, G. A. Sawatzky, M. Campagna, O. Gunnarsson, and K. Schönhammer, Phys. Rev. B **30**, 1777 (1984).
[31]J. C. Fuggle, F. U. Hillebrecht, Z. Zolnierek, R. Lässer, Ch. Freiburg, O. Gunnarsson, and K. Schönhammer, Phys. Rev. B **27**, 7330 (1983), and references therein.
[32]B. T. Thole, G. v.d. Laan, J. C. Fuggle, G. A. Sawatzky, R. C. Karnatak, J.-M. Esteva, and B. Lengeler, J. Phys. F (to be published).
[33]G. Strasser and F. P. Netzer, J. Vac. Sci. Technol. A **2**, 826 (1984).
[34]E. Wuilloud, B. Delley, W.-D. Schneider, and Y. Baer, Phys. Rev. Lett. **53**, 202 (1984).
[35]A. Fujimori, Phys. Rev. B **27**, 3992 (1983); **28**, 2881 (1983); **28**, 4489 (1983).
[36]G. H. Dieke and H. M. Crosswhite, Appl. Opt. **2**, 675 (1963).
[37]U. Fano, Phys. Rev. **124**, 1866 (1961).
[38]G. Kaindl, W. D. Brewer, G. Kalkowski, and F. Hotzberg, Phys. Rev. Lett. **51**, 2056 (1983).
[39]The first attempt to use he $M_{4,5}$ XAS lines for studies of mixed valence appears to be that of D. O. Sewell, E. A. Stewardson, and J. E. Wilson, J. Phys. B **6**, 2184 (1973), but some of those experimental results seem to be in error. Other work includes Ref. 3.
[40]F. H. Combley, E. A. Stewardson, and J. E. Wilson, J. Phys. B **1**, 120 (1968).